

Absence of Supercritical Behavior in Gapped Graphene with Short-range Impurity Scattering

Stepan Grinek^{1,4}, Zhou Li², Jie Chen^{1,4*}, Qinwei Shi³, Frank Marsiglio²

¹*Electrical and Computer Engineering, University of Alberta, Alberta, Canada T6G 2V4*

²*Department of Physics, University of Alberta, Canada T6G 2V4*

³*Hefei National Laboratory for Physical Sciences at Microscale,*

University of Science and Technology of China, Hefei 230026, China and

⁴*National Research Council/National Institute of Nanotechnology, Alberta, Canada T6G 2M9**

(Dated: November 8, 2018)

We show that the changes in the electronic density of states (DOS) in graphene induced by localized impurities (single, double and multiple) are significantly different from those caused by the long-range Coulomb potential. We focus on gapped graphene; a bound state is present within the gap, with a certain amount of spectral weight. As the coupling to the impurity increases, the state lowers in energy and approaches the lower continuum valence band. The spectral weight of this state does not transform into a resonance state in the valence band, so no unusual screening effects related to a redistribution of DOS in the continuum is observed. In terms of the continuous Dirac limit, this phenomenon is a consequence of the absence of the “potential bump” at infinity, which is present in the potential of the effective Schrödinger equation for graphene with long-range Coulomb impurity potential. The states induced by short-range impurity scattering in graphene, therefore, have distinctly different properties compared with the long-range potential case. These properties closely resemble the case of a short-range single impurity in other bipartite lattices, such as square, body-centered cubic, and simple cubic lattices. For these bipartite lattices, there is always a localized bound state with energy in the band gap for the entire range of on-site coupling strengths. In all cases the energy of these states asymptotically approaches the edge of the valence band as the magnitude of the coupling strength increases, but never crosses it.

PACS numbers: 81.05.Uw, 71.55.-i, 71.23.-k

I. INTRODUCTION

Graphene has been used as an analog case to study relativistic phenomena in heavy atoms because the critical charge for the Dirac fermions in graphene is of the order of unity¹. Upon introduction of a single charge impurity into an otherwise perfect lattice, a bound state appears within the mass gap that separates the original Dirac cones^{2,3}. As one tunes the coupling strength of this charge impurity to larger values, eventually a critical charge condition is achieved whereby the energy of the bound states passes into the continuum. In gapped graphene, this crossover has implications for the screening properties of the electron gas.¹ The wave function of such a bound state decays exponentially with the distance from the charge. As the coupling strength becomes supercritical, the screening effect is sufficiently strong that the observed effective charge is reduced by almost 4 elementary units compared with the unscreened case.¹ This phenomenon is similar to what happens in atomic physics when the elementary charge is around 170.⁴ The shape of the cloud of screening charge closely follows the shape of the so called “critical state” just before it merges with the continuum of the valence band. A couple of questions arise: i) Is there a change in the electronic structure that depends on the range of potential? ii) What are the properties that define whether the impurity potential strength is critical or not?

The paper is organized as follows. In the next section we obtain the predictions of the long-wavelength Dirac

formalism in the case of one or few short-range impurities. In the third section, after we briefly review the Green functions on the lattice pertinent to the honeycomb lattice, we obtain analytical results for one and two impurities on the graphene lattice. In the fourth section, we generalize our results for multiple short-ranged impurities, and then we close with the conclusion.

II. DIRAC EQUATION WITH SPHERICAL WELL

The motion of an electron with a fixed full (pseudo-spin plus orbital) angular momentum in a circularly symmetric potential $U(r)$ is:

$$\begin{aligned} (E - U(r) - m)A(r) - (\partial_r + \frac{j}{r})B(r) &= 0, \\ (\partial_r - \frac{j}{r})A(r) + (E - U(r) + m)B(r) &= 0, \end{aligned} \quad (1)$$

where, for definiteness, $U(r) = V\theta(a - r)$, where $\theta(x)$ is a Heaviside step function, a is the radius of the well, and V is negative (positive) for a well (barrier). The full wave function is¹:

$$\Psi_C(r, \phi) = \frac{1}{\sqrt{r}} \left\{ \begin{array}{l} e^{-i(j-1/2)\phi} A(r) \\ ie^{-i(j+1/2)\phi} B(r) \end{array} \right\}. \quad (2)$$

Here j is an eigenvalue of angular momentum $J_z = L_z + \frac{1}{2}\sigma_z$, and C can refer to either the A or B sublattice. To

solve Eq. (1), one can express $B(r)$ in terms of $A(r)$:

$$B(r) = \frac{\frac{j}{r}A(r) - A'(r)}{E - V + m}. \quad (3)$$

In what follows, we will discuss the case when the energy level is at either gap edge; for negative (positive) V this is the lower (upper) edge. The solutions inside the well are:

$$A(r) = C_1 \sqrt{r} \sqrt{\frac{E+m-V}{E-m-V}} J_{j-1/2}(\sqrt{(E-V)^2 - m^2}r),$$

$$B(r) = C_1 \sqrt{r} J_{j+1/2}(\sqrt{(E-V)^2 - m^2}r). \quad (4)$$

The solutions outside the well are:

$$A(r) = C_2 \sqrt{r} \sqrt{\frac{E+m}{E-m}} K_{j-1/2}(\sqrt{m^2 - E^2}r),$$

$$B(r) = -iC_2 \sqrt{r} K_{j+1/2}(\sqrt{m^2 - E^2}r), \quad (5)$$

where $J_\alpha(x)$ is a Bessel function of the first kind, $K_\alpha(x)$ is a modified Bessel function of the second kind chosen to satisfy the boundary condition at infinity. The equation for the energy levels is:

$$\frac{\sqrt{\frac{E+m-V}{E-m-V}} J_{j-1/2}(\sqrt{(E-V)^2 - m^2}a)}{J_{j+1/2}(\sqrt{(E-V)^2 - m^2}a)} = \frac{i \sqrt{\frac{E+m}{E-m}} K_{j-1/2}(\sqrt{m^2 - E^2}a)}{K_{j+1/2}(\sqrt{m^2 - E^2}a)}. \quad (6)$$

For a solution to exist, the terms on the left-hand side and on the right-hand side must be either pure imaginary or pure real numbers. This means, that for $-m \leq E \leq 0$, and with $V < 0$, then we require that $(E - V)^2 > m^2$ for a solution. We are primarily interested in negative values of V .

We are interested also in what sequence the levels will merge into the continuum, depending on their angular momentum. One can numerically analyze Eq. (6) but for the sake of clarity we will analyze the effective Schrodinger equation for $A(r)$, obtained from the system (1):

$$-A''(r) + \left[\frac{j^2 - j}{r^2} - (E - V)^2 + m^2 \right] A(r) = 0 \quad (7)$$

This is a wave equation for a particle in a potential with functional form $\frac{j^2 - j}{r^2} - (E - V)^2 + m^2$ at zero energy. Obviously, for states with a higher value of $j^2 - j$, the potential curve is higher, particularly near the origin; states with a higher value of j will merge into the continuum for larger values of $|V|$. Another way of looking at the properties of the wave function as these solutions merge into the continuum is to find asymptotic solutions outside the well when $E \rightarrow -m + 0$:

$$|\Psi_A|^2 = |A(r)|^2/r \simeq \frac{C_2^2}{r} \frac{E+m}{E-m} \frac{1}{\sqrt{m^2 - E^2}} e^{-2\sqrt{m^2 - E^2}r}$$

$$|\Psi_B|^2 = |B(r)|^2/r \simeq -\frac{C_2^2}{r} \frac{1}{\sqrt{m^2 - E^2}} e^{-2\sqrt{m^2 - E^2}r}. \quad (8)$$

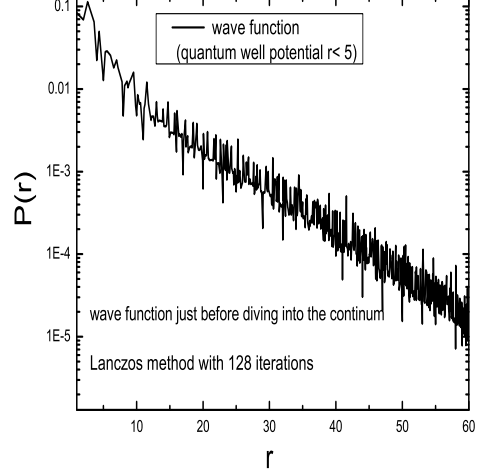


FIG. 1: Asymptotic behavior of wave function close to the band edge for quantum well potential.

Note that the wave function disappears on A-sites and Ψ_B becomes non-normalizable when $E = -m$.

As we will see from the following, the Dirac approximation for graphene gives correct predictions for electronic properties at the critical coupling strength, because the energies involved are right at the boundary of the valence band, where the linear dispersion is most accurate.

III. ANALYTICAL RESULTS FOR ONE AND TWO IMPURITIES ON THE LATTICE

A. Lattice Green function

The Hamiltonian of a free electron in the two-dimensional graphene lattice, using the tight binding model is,

$$H_0 = -t \sum_{j,\delta} (a_j^\dagger b_{j+\delta} + b_{j+\delta}^\dagger a_j) + m \sum_{\mathbf{i}} (a_{\mathbf{i}}^\dagger a_{\mathbf{i}} - b_{\mathbf{i}}^\dagger b_{\mathbf{i}}), \quad (9)$$

where a_j^\dagger is the creation operator of an electron on the A-atom site labeled j in the honeycomb lattice, and $b_{j+\delta}$ represents the annihilation of an electron on the neighboring B-atom site labeled $j+\delta$. Here δ denotes the three vectors that connect an A-atom site to its three nearest neighboring B-atom sites. The parameters t and m represent the nearest neighbor hopping probability and the mass differentiating the A and B sublattices, respectively. The Hamiltonian in k-space can be written as:

$$\hat{H}_0 = \begin{pmatrix} m & \phi_k \\ \phi_k^* & -m \end{pmatrix}, \quad (10)$$

where we have adopted the standard spinor notation for the A and B sublattice components of the wave function. Here, $\phi_k = -te^{-ik_x a}(1 + 2\cos(k_y\sqrt{3}a/2)e^{ik_x a3/2})$, where a is the distance between neighboring atoms. The eigenvalues are

$$\epsilon_{\mathbf{k},\pm} = \pm\sqrt{t^2(1 + 4c_y^2 + 4c_x c_y) + m^2}, \quad (11)$$

where $c_x \equiv \cos 3k_x a/2$ and $c_y \equiv \cos \sqrt{3}k_y a/2$. The Green functions in k -space can be obtained straightforwardly as

$$\mathbb{G}_0(\mathbf{k}, i\omega_n) = \begin{bmatrix} G_{AA}^0(\mathbf{k}, i\omega_n) & G_{AB}^0(\mathbf{k}, i\omega_n) \\ G_{BA}^0(\mathbf{k}, i\omega_n) & G_{BB}^0(\mathbf{k}, i\omega_n) \end{bmatrix}, \quad (12)$$

where $i\omega_n = i\pi T(2n - 1)$ (with n an integer) are the Fermion Matsubara frequencies (T is the temperature), and each component is given by

$$\begin{aligned} G_{AA}^0(\mathbf{k}, i\omega_n) &= \frac{i\omega_n + \mu + m}{(i\omega_n + \mu)^2 - \epsilon_k^2} \\ G_{BB}^0(\mathbf{k}, i\omega_n) &= \frac{i\omega_n + \mu - m}{(i\omega_n + \mu)^2 - \epsilon_k^2} \\ G_{AB}^0(\mathbf{k}, i\omega_n) &= \frac{\phi_k^*}{(i\omega_n + \mu)^2 - \epsilon_k^2} \\ G_{BA}^0(\mathbf{k}, i\omega_n) &= \frac{\phi_k}{(i\omega_n + \mu)^2 - \epsilon_k^2}. \end{aligned} \quad (13)$$

We have added μ , the chemical potential, for completeness, and the superscript '0' serves to remind us that these Green functions are applicable to the clean lattice, i.e. without impurity scattering. The lattice Green functions in real space can be obtained by Fourier transform from the above Green's functions:

$$\mathbb{G}_0(l, j, i\omega_n) = \begin{bmatrix} G_{AA}^0(l, j, i\omega_n) & G_{AB}^0(l, j, i\omega_n) \\ G_{BA}^0(l, j, i\omega_n) & G_{BB}^0(l, j, i\omega_n) \end{bmatrix},$$

where

$$G_{AA}^0(l, j, i\omega_n) = \frac{(\omega + \mu + m)}{4\pi^2} \int_{-\pi}^{\pi} du \int_{-\pi}^{\pi} dv \quad (14)$$

$$\times \frac{e^{iu(l_x - j_x)} e^{-iv(l_x - j_x)} e^{i2v(l_y - j_y)}}{(\omega + \mu)^2 - m^2 - t^2(1 + 4\cos^2 v + 4\cos u \cos v)},$$

$$G_{AB}^0(l, j, i\omega_n) = -\frac{1}{4\pi^2} \int_{-\pi}^{\pi} du \int_{-\pi}^{\pi} dv \quad (15)$$

$$\times \frac{e^{iu(l_x - j_x)} e^{-iv(l_x - j_x)} e^{i2v(l_y - j_y)} (1 + 2e^{-iu} \cos v)}{(\omega + \mu)^2 - m^2 - t^2(1 + 4\cos^2 v + 4\cos u \cos v)}.$$

The remaining components are readily obtained through the relations $G_{BB}^0(l, j, i\omega_n) = G_{AA}^0(l, j, i\omega_n, m \rightarrow -m)$ and, for the off-diagonal components, $G_{BA}^0(l, j, i\omega_n) = [G_{AB}^0(l, j, i\omega_n)]^*$. Through the analytic continuation, $i\omega_n \rightarrow \omega + i\delta$, we obtain the Green functions slightly above the real axis, corresponding to the retarded Green function. For the particular case of $l = j$ (an on-site

Green function), we can obtain the diagonal components analytically. From now on we set $t=1$, which means that all energies are measured in units of the hopping energy. The result for G_{AA}^0 is (we set $\mu = 0$ for simplicity, and use the definition $E^2 = |\omega^2 - m^2|$):

(i) For $0 < E < 1, \omega^2 - m^2 < 0$,

$$\begin{aligned} \text{Re}[G_{AA}^0(l, l, \omega)] &= -\frac{(\omega + m)}{\pi} \frac{2}{\sqrt{(\sqrt{E^2 + 1})^3 \sqrt{E^2 + 9}}} \\ &\times F\left(\frac{\pi}{2}, \frac{1}{2} \sqrt{\frac{-(E^4 + 12E^2 - 6)}{(\sqrt{E^2 + 1})^3 \sqrt{E^2 + 9}}} + 2\right), \end{aligned}$$

$$\text{Im}[G_{AA}^0(l, l, \omega)] = 0.$$

(ii) For $0 < E < 1, \omega^2 - m^2 > 0$

$$\begin{aligned} \text{Re}[G_{AA}^0(l, l, \omega)] &= -\frac{(\omega + m)}{\pi} \frac{4}{\sqrt{3 - E} [\sqrt{(E + 1)}]^3} \\ &\times F\left(\frac{\pi}{2}, \sqrt{\frac{[3 + E](1 - E)^3}{[3 - E](E + 1)^3}}\right), \end{aligned}$$

$$\begin{aligned} \text{Im}[G_{AA}^0(l, l, \omega)] &= -\frac{2(\omega + m)}{\pi} \frac{1}{\sqrt{3 - E} [\sqrt{(E + 1)}]^3} \\ &\times F\left(\frac{\pi}{2}, \sqrt{\frac{16E}{[3 - E](E + 1)^3}}\right). \end{aligned}$$

(iii) for $1 < E < 3$

$$\text{Re}[G_{AA}^0(l, l, \omega)] = \frac{(\omega + m)}{2\pi} \frac{1}{\sqrt{E}} \times F\left(\frac{\pi}{2}, \sqrt{\frac{(E + 3)(E - 1)^3}{16E}}\right),$$

$$\text{Im}[G_{AA}^0(l, l, \omega)] = -\frac{(\omega + m)}{2\pi} \frac{1}{\sqrt{E}} F\left(\frac{\pi}{2}, \sqrt{\frac{[3 - E](E + 1)^3}{16E}}\right).$$

(iv) for $E > 3$

$$\begin{aligned} \text{Re}[G_{AA}^0(l, l, \omega)] &= \frac{2(\omega + m)}{\pi} \frac{1}{\sqrt{(E + 3)(E - 1)^3}} \\ &\times F\left(\frac{\pi}{2}, \sqrt{\frac{16E}{(E + 3)(E - 1)^3}}\right), \end{aligned}$$

$$\text{Im}[G_{AA}^0(l, l, \omega)] = 0.$$

In these expressions we have used $F(\frac{\pi}{2}, x) \equiv \int_0^{\pi/2} (1 - x \sin^2 \theta)^{-1/2} d\theta$, which is a complete elliptic integral of the first kind (also denoted as $K(x)$).⁵

B. Analytical formalism

We start with the equation

$$\hat{G} = (\hat{I} - \hat{G}^0 \hat{V})^{-1} \hat{G}^0, \quad (16)$$

where \hat{G} denotes a matrix where different rows (and columns) correspond to different lattice sites (an explicit example below will make this clearer, see also Ref. 6).

As an example, we consider the specific case with two on-site impurities located at the sites labeled 0 and 1 (without loss of generality, we number the first atom on the A sublattice as 0, and we number the first atom on the B sublattice as 1; since the lattice is bi-partite, A -atoms are denoted by even numbers, and B -atoms are denoted by odd numbers). The $\hat{I} - \hat{G}_0 \hat{V}$ matrix is then written explicitly as

$$\hat{I} - \hat{G}_0 \hat{V} = \begin{pmatrix} 1 - VG_{00}^0 & -VG_{01}^0 & 0 & 0 & \dots \\ -VG_{10}^0 & 1 - VG_{11}^0 & 0 & 0 & \dots \\ -VG_{20}^0 & -VG_{21}^0 & 1 & 0 & \dots \\ -VG_{30}^0 & -VG_{31}^0 & 0 & 1 & \dots \\ \dots & \dots & \dots & \dots & \dots \end{pmatrix}, \quad (17)$$

where now the subscripts refer to the two site indices (previously written as arguments in, say, Eq. (14)), and V is the strength of the impurity potential at both sites. Then

$$G_{jj} = \sum_k (I - G^0 V)_{jk}^{-1} G_{kj}^0 = C_{kj} G_{kj}^0 / \Delta, \quad (18)$$

where C is a cofactor in the matrix (17), and Δ is the determinant of $\hat{I} - \hat{G}_0 \hat{V}$. The factor C_{kj} is $(-1)^{i+j}$ times the determinant of the original matrix excluding the k -th row and j -th column. Eq. (18) can be expressed as:

$$G_{jj} = C_{kj} G_{kj}^0 / \Delta \quad (19)$$

$$= \left[\sum_k C_{jj} G_{jj}^0 + \sum_{k \leq l, k \neq j} C_{kj} G_{kj}^0 + \sum_{k > l, k \neq j} C_{kj} G_{kj}^0 \right] / \Delta.$$

Here the number l is given by the number of sites occupied by an impurity.

For $j > l$ (away from the impurities), $\sum_{k > l, k \neq j} C_{kj} G_{kj}^0 = 0$ in Eq. (19). In this case Eq. (19) becomes:

$$G_{jj} = \sum_k C_{kj} G_{kj}^0 / \Delta = \left[C_{jj} G_{jj}^0 + \sum_{k \leq l, k \neq j} C_{kj} G_{kj}^0 \right] / \Delta. \quad (20)$$

The cofactor C_{jj} is equal to Δ , and therefore

$$G_{jj} = G_{jj}^0 + \left[\sum_{k \leq l, k \neq j} C_{kj} G_{kj}^0 \right] / \Delta. \quad (21)$$

Note that when $\omega = -m$, $G_{00}^0(\omega + i\delta) \sim 0$.

C. Single impurity scattering

When there is only one impurity at any A -atom site, the Hamiltonian is given by $\hat{H} = \hat{H}_0 + \hat{H}_1$, where $\hat{H}_1 = \hat{V}$.

The corresponding Green functions corresponding to the two Hamiltonians are $\hat{G}_0(z) = (z - \hat{H}_0)^{-1}$ and $\hat{G}(z) = (z - \hat{H})^{-1}$. By using the T-matrix expansion, we obtain the Green function in the presence of a single impurity:

$$G_{ij} = G_{ij}^0 + \frac{G_{i0}^0 V G_{0j}^0}{1 - V G_{00}^0}. \quad (22)$$

The local density of states (LDOS) at any position on the graphene lattice is defined by the imaginary part of Green function:

$$\rho(j, j, \omega) = -\frac{1}{\pi} \text{Im} G_{jj}(\omega + i\delta), \quad (23)$$

and we have restored the explicit frequency dependence for clarity.

The local density of states at the impurity site is $\rho(0, 0, \omega) = -\frac{1}{\pi} \text{Im} \left(\frac{G_{00}^0(\omega + i\delta)}{1 - V G_{00}^0(\omega + i\delta)} \right)$. The position of the bound state in the gap is determined by the solution of the equation $1 - V G_{00}^0(\omega + i\delta) = 0$. At the lower band edge where $\omega \rightarrow -m$, $G_{00}^0(\omega + i\delta) \sim \omega + m = 0$. Therefore, inspection of the above equation suggests that no solution exists, unless $V \rightarrow -\infty$. This observation implies that for any V the bound state will not merge into the lower continuum, i.e. no bound state energy crosses the edge at $\omega = -m$. For a single impurity on a B -atom site, the same remarks apply for a positive impurity potential, and the upper band edge plays the role previously played by the lower band edge.

To understand how the bound state approaches the continuum band edge, we use the asymptotic expansion of the complete elliptic integral of the first kind⁵ to get

$$G_{00}(\omega + i\delta) \simeq \frac{K(\omega + m) \ln |\omega + m|}{1 - V K(\omega + m) \ln |\omega + m|}; \quad (24)$$

where $K = \frac{1}{\sqrt{3\pi}}$. By expanding the Green function near $\omega = -m$ we obtain a pole with spectral weight $a_0 = -K\omega_1^2 \ln \omega_1$, where $\omega_1 \equiv \omega + m$ is the solution of

$$1 - V K \omega_1 \ln \omega_1 = 0. \quad (25)$$

It is clear that as $\omega_1 \rightarrow 0$ a solution will only occur as $V \rightarrow -\infty$, and the residue corresponding to that solution approaches zero.

At the other extreme, for a very weak (negative) impurity potential, a similar expansion near $\omega \sim m$ gives a bound state energy asymptotically approaching the upper band edge (let $\omega_2 \equiv m - \omega$):

$$\omega_2 \approx \exp \frac{-1}{2mK|V|}. \quad (26)$$

The spectral weight approaches zero here as well, as $a_0 = 2mK\omega_2 \ln^2 \omega_2$, which also goes to zero as the upper band edge is approached.

To summarize the results of this section, we showed that, as the (negative) impurity potential decreases from

zero towards negative infinity, the frequency of the pole migrates from $+m$ (upper band edge) to $-m$ (lower band edge). As this occurs, the spectral weight first starts from zero, grows to some maximum, and then decreases again to zero, as the strength of the potential varies from zero to negative infinity.

IV. TWO OR MORE IMPURITY SCATTERING

A. Exact solution for two impurities

We now consider the two-impurity case, with one on an A -site, $(0, 0)$, and the second on a B -site $\mathbf{i}(i_x, i_y)$. The Hamiltonian is

$$\hat{H} = \hat{H}_0 + \hat{V} + \hat{V}_2 = \hat{H}_1 + \hat{H}_2,$$

where $\hat{H}_1 = \hat{H}_0 + \hat{V}$ as in the single impurity case. The Green functions G^0 , G^1 and G correspond to \hat{H}_0 , \hat{H}_1 and \hat{H} , respectively. The T-matrix for this case is

$$\hat{T} = \hat{H}_2 + \hat{H}_2 \hat{G}^1 \hat{H}_2 + \dots$$

Therefore, the Green function becomes

$$G_{jk} = G_{jk}^1 + \frac{G_{ji}^1 V_2 G_{ik}^1}{1 - V_2 G_{ii}^1}.$$

In fact, for the many-impurity case, the T-matrix method can be used in a recursive way,

$$\hat{G}^n = \hat{G}^{n-1} + \hat{G}^{n-1} \hat{T}_n \hat{G}^{n-1},$$

where

$$(T_n)_{i,i} = \frac{V_n}{1 - V_n (G^{n-1})_{i,i}}.$$

To compute the local density of states at site $(0, 0)$, we need $G_{00}(\omega)$ (for simplicity we suppress the $i\delta$):

$$\begin{aligned} & G_{00}(\omega) \\ &= G_{00}^1(\omega) + \frac{G_{01}^1(\omega) V_2 G_{10}^1(\omega)}{1 - V_2 G_{11}^1(\omega)} \\ &= \frac{G_{00}^0(\omega) [1 - V_2 G_{11}^0(\omega)] + V_2 |G_{01}^0(\omega)|^2}{[1 - V_2 G_{11}^0(\omega)] [1 - V G_{00}^0(\omega)] - V V_2 |G_{01}^0(\omega)|^2} \\ &= \frac{F(\omega)}{(\omega - \omega_0) + i\delta}, \end{aligned} \quad (27)$$

where ω_0 is the energy of the pole, and $F(\omega)$ accounts for the remaining (non-singular) frequency dependence. The actual pole position is the solution of

$$[1 - V_2 G_{11}^0(\omega_0)] [1 - V G_{00}^0(\omega_0)] = V V_2 |G_{01}^0(\omega_0)|^2, \quad (28)$$

and the spectral weight is given by $F(\omega_0)$.

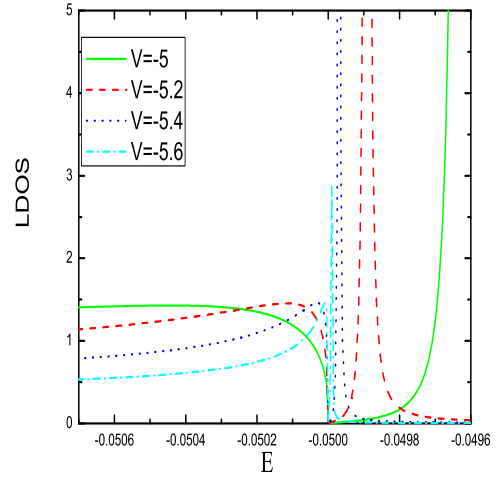
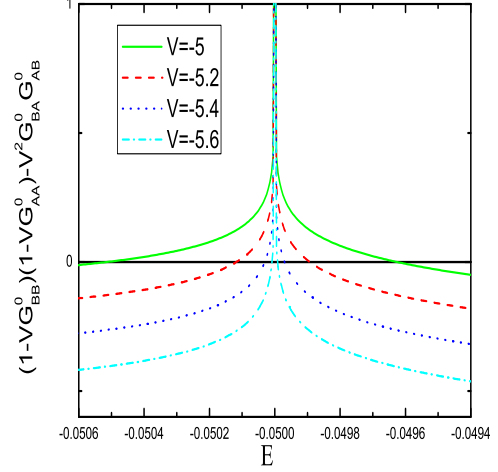


FIG. 2: (color online) The behavior of LDOS at the valence band edge for two impurities.

Then the Green function in the case $V_2 = V$ is given by

$$G_{00}(\omega) = \frac{G_{00}^0(1 - V G_{11}^0) + V |G_{01}^0|^2}{(1 - V G_{00}^0)(1 - V G_{11}^0) - V^2 |G_{01}^0|^2}, \quad (29)$$

Keeping the leading term for G_{11}^0 , we find

$$G_{11}^0(\omega) \simeq -2mK \ln \omega, \quad (30)$$

$$a_0 = \frac{C \omega_1}{2mK}, \quad (31)$$

where the quantity $C = |G_{01}^0|^2$ is finite near $\omega = -m$, and we get the result near the bottom of the upper band:

$$a_0 = 2mK \omega_2 \ln^2 \omega_2, \quad (32)$$

The definitions of ω_1, ω_2 are the same as in the case of single impurity scattering discussed in the previous section. The conclusion is the same: as the strength of the impurity interaction increases, the pole moves towards the top of the bottom band, but never crosses it. Instead, the residue associated with the pole decreases to zero. The key difference with the Coulomb case is that these are short range impurities, and this leads to qualitatively different behaviour.

B. Long-range asymptotes of the Green functions for a large number of impurities

In this subsection we generalize to some extent the results obtained in the previous sections. We find the long-range asymptotic behavior of the Green function in the case of multiple impurities located inside a finite area of the graphene sheet. As a particular case this discussion includes the circular well, discussed in the Dirac approximation, at the beginning of the article in Section II. Knowing these Green functions' asymptotes we show that the spectral weight of the state near the band edge (on the verge of entering into the lower continuum) is zero and the screening charge is not significantly reshaped by this state.¹

We rewrite Eq. (21):

$$G_{\mathbf{R}\mathbf{R}} = G_{\mathbf{R}\mathbf{R}}^0 + \left[\sum_{r \leq a} C_{\mathbf{r}\mathbf{R}} G_{\mathbf{r}\mathbf{R}}^0 \right] / \Delta. \quad (33)$$

Here we introduced the following notation: R is the distance from the center of the area in which the impurities are confined; we will call this area the ‘‘potential well’’; \mathbf{R} corresponds to the site index outside the well; a is the radius of the well; r and r' are the distances inside the circle of radius a , and \mathbf{r} is the index of the site inside the well.

The second term in Eq. (33) represents the change induced by the impurity and is responsible for the spectral weight of the bound state. Assuming $R \gg a$, the following conclusions can be made about the second term. Δ does not depend on R , but $C_{\mathbf{r}\mathbf{R}}$ depends on R , and $C_{\mathbf{r}\mathbf{R}} \sim G_{\mathbf{r}\mathbf{R}}^0$, as the determinant $C_{\mathbf{r}\mathbf{R}}$ contains only one row with $G_{\mathbf{r}\mathbf{R}}^0$.

Considering the sum over \mathbf{r} in $\sum_{r \leq a} C_{\mathbf{r}\mathbf{R}} G_{\mathbf{r}\mathbf{R}}^0$ we see that the r dependency comes only from the phase $\vec{k} \cdot (\vec{R} - \vec{r})$ in the exponent of the integrands (14, 15). At the energies near the band edge $\omega \rightarrow -m$, the part $\vec{k} \cdot \vec{r}$ can be neglected, as the small k 's produce most of the integral value and $\vec{k} \cdot \vec{r}$ does not vary significantly near the Dirac point. Therefore,

$$\sum_{r \leq a} C_{\mathbf{r}\mathbf{R}} G_{\mathbf{r}\mathbf{R}}^0 \sim (G_{\mathbf{0}\mathbf{R}}^0)^2. \quad (34)$$

The spatial dependance of the second term in $G_{\mathbf{R}\mathbf{R}}$ is determined by the $(G_{\mathbf{0}\mathbf{R}}^0)^2$, where $\mathbf{0}$ denotes some (arbitrary chosen) site in the impurity-occupied area. To determine the asymptotic behaviour of $G_{\mathbf{0}\mathbf{R}}^0$, we use the method of stationary phase (see problem 5.2 in⁷), and get

$$G_{\mathbf{0}\mathbf{R}}^0(\omega \rightarrow -m) \sim \frac{\exp(-R\sqrt{\delta E})}{(\delta E)^{1/4}\sqrt{R}}, \quad (35)$$

where $\delta E = m^2 - \omega^2$. Thus $G_{\mathbf{R}\mathbf{R}} \sim \frac{\exp(-2R\sqrt{\delta E})}{(\delta E)^{1/2}R}$, in qualitative agreement with the asymptotic behavior predicted by the Dirac equation (8). As we can see from the standard definition of the Green function⁷:

$$G_{\mathbf{R}\mathbf{R}'}(\omega) = \sum_n \frac{\psi_n(\mathbf{R})\psi_n(\mathbf{R}')^*}{\omega - \omega_n} + \int dc \frac{\psi_c(\mathbf{R})\psi_c(\mathbf{R}')^*}{\omega - \omega_c} \quad (36)$$

when $\omega \rightarrow \omega_n$ the r -dependency of $G_{\mathbf{R}\mathbf{R}}(\omega)$ coincides with $\psi_n(\mathbf{R})\psi_n(\mathbf{R}')^*$ and we can judge if the state that is potentially crossing the band edge into the continuum is normalizable. In our case as $\delta E \rightarrow 0$ the sum of $G_{\mathbf{R}\mathbf{R}}$ over \mathbf{R} in the plane diverges, and so does the sum $\psi_n(\mathbf{R})\psi_n(\mathbf{R}')^*$ in the infinite lattice for any finite normalizing factor. Hence the state merging into the continuum can be called non-normalizable or extended and as such has zero spectral weight (in the thermodynamic limit). This confirms our conclusion that there is no such phenomenon like supercritical screening in the case of a localized potential (as opposed to a Coulomb potential) in graphene.

V. CONCLUSIONS

Our results are in agreement with common intuition developed in the physics of shallow states in semiconductors. In particular it is not only a feature peculiar to gapped graphene that properties of the states near the band edge are strongly dependent on the long range ‘‘tail’’ of the impurity potential.⁸ In general, the effective mass approach (mostly determined by long-range properties of a system) is in good agreement with exact numerical methods for the energies near the band edge. It is exactly near the band edge where the Coulomb tail becomes important while it is negligible in computations related to deep levels.⁹ As illustrated in Section II, in the continuum limit a potential barrier emerges in the effective potential at large distances, due to the squaring of the Coulomb potential. Because of the two sublattices, a similar ‘squaring’ occurs when the problem is solved on a lattice, and lattice Green functions are utilized.¹⁰

* Electronic address: jc65@ualberta.ca

- ¹ V. M. Pereira, V. N. Kotov, and A. H. Castro-Neto, "Supercritical Coulomb Impurities in Gapped Graphene," *Physical Review E*, **78**, 8, 2008, pp. 085101
- ² Peres, N. M. R., Guinea, F. Castro Neto, A. H. "Electronic properties of two-dimensional carbon", *Annals of Physics* **321**, 1559 (2006)
- ³ S. Y. Zhou, G. -H. Gweon, A. V. Fedorov, P. N. First, W. A. De Heer, D. -H. Lee, F. Guinea, A. H. Castro Neto and A. Lanzara, *Nature Mater.* **6**, 770 (2007).
- ⁴ Ya B Zeldovich, V S Popov, 1972 *Sov. Phys. Usp.* **14** 673-694
- ⁵ M. Abramowitz and I.A. Stegun, *Handbook of Mathematical Functions* (Dover, New York, 1972).
- ⁶ J. Callaway, A.J.Hughes, *Phys. Rev.* **156**, 860, (1967).
- ⁷ Economou E.N., *Green Functions in Quantum Physics*, <http://www.springerlink.com/content/j75035r1618442q2>
- ⁸ S. Pantelides, *Rev. Mod. Phys.* **50**, 797 (1978)
- ⁹ C. Rodriguez, S. Brand, M. Jaros, *J. Phys. C: Solid St. Phys.*, **13**, L333 (1980)
- ¹⁰ T. Morita, T. Horiguchi, *J. Math. Phys* **13**, 8, (1972) *Rev. Lett.* **99**, 236801 (2007).

